Molecular Therapy
Original Article

CAR T Cells Targeting MISIIR for the Treatment of Ovarian Cancer and Other Gynecologic Malignancies

Alba Rodriguez-Garcia,[1,2,3] Prannda Sharma,[1,2,3] Mathilde Poussin,[1,2,3] Alina C. Boesteanu,[3] Nicholas G. Minutolo,[1,2,3] Sarah B. Gitto,[1,2,3] Dalia K. Omran,[1] Matthew K. Robinson,[4,6] Gregory P. Adams,[4,7] Fiona Simpkins,[5] and Daniel J. Powell, Jr.[1,2,3]

[1]Ovarian Cancer Research Center, Department of Obstetrics and Gynecology, Perelman School of Medicine, University of Pennsylvania, Philadelphia, PA 19104, USA; [2]Department of Pathology and Laboratory Medicine, Abramson Cancer Center, University of Pennsylvania, Philadelphia, PA 19104, USA; [3]Center for Cellular Immunotherapies, Abramson Cancer Center, University of Pennsylvania, Philadelphia, PA 19104, USA; [4]Developmental Therapeutics Program, Fox Chase Cancer Center, Philadelphia, PA 19111, USA; [5]Ovarian Cancer Research Center, Division of Gynecology Oncology, Department of Obstetrics and Gynecology, University of Pennsylvania, Philadelphia, PA 19104, USA

The prognosis of patients diagnosed with advanced ovarian or endometrial cancer remains poor, and effective therapeutic strategies are limited. The Müllerian inhibiting substance type 2 receptor (MISIIR) is a transforming growth factor β (TGF-β) receptor family member, overexpressed by most ovarian and endometrial cancers while absent in most normal tissues. Restricted tissue expression, coupled with an understanding that MISIIR ligation transmits apoptotic signals to cancer cells, makes MISIIR an attractive target for tumor-directed therapeutics. However, the development of clinical MISIIR-targeted agents has been challenging. Prompted by the responses achieved in patients with blood malignancies using chimeric antigen receptor (CAR) T cell therapy, we hypothesized that MISIIR targeting may be achieved using a CAR T cell approach. Herein, we describe the development and evaluation of a CAR that targets MISIIR. T cells expressing the MISIIR-specific CAR demonstrated antigen-specific reactivity *in vitro* and eliminated MISIIR-overexpressing tumors *in vivo*. MISIIR CAR T cells also recognized a panel of human ovarian and endometrial cancer cell lines, and they lysed a battery of patient-derived tumor specimens *in vitro*, without mediating cytotoxicity of a panel of normal primary human cells. In conclusion, these results indicate that MISIIR targeting for the treatment of ovarian cancer and other gynecologic malignancies is achievable using CAR technology.

INTRODUCTION

Ovarian cancer (OC) is the most lethal of all gynecologic malignancies and the fifth leading cause of cancer-related death in women. The initial response to standard therapies is seldom durable and recurrent disease is often refractory to subsequent treatment and ultimately fatal. The most frequent cancer of the genital tract is endometrial cancer (EC), in which there is a poor prognosis for patients with disseminated disease (https://seer.cancer.gov/statfacts). Therefore, there remains a dire need to develop novel therapeutic strategies that are both effective and safe to improve survival in women with advanced ovarian and endometrial cancers.

The Müllerian inhibiting substance type II receptor (MISIIR), also known as anti-Müllerian hormone type II receptor (AMHR2), is a transforming growth factor β (TGF-β) receptor family member involved in the regression of the Müllerian ducts (precursors to the uterus, fallopian tubes, and vagina) in male embryos. This action is exerted through a specific ligand named Müllerian inhibiting substance (MIS, or AMH) that triggers a downstream signaling cascade inducing cell cycle arrest and apoptosis.[1] MISIIR is overexpressed in the vast majority of epithelial OCs and endometrial carcinomas, as well as other gynecologic malignancies, including uterine sarcoma and cervical carcinoma.[2–7] MISIIR expression is also reported in several non-gynecologic cancers such as breast, prostate, lung, or ocular melanoma.[8–11]

In line with its natural function, MIS signaling causes growth inhibition of MISIIR-expressing cancer cells *in vitro* and *in vivo*,[3,6,8,12–15] as well as primary cellular isolates from the ascites of OC patients.[2] This makes recombinant MIS protein an attractive potential therapeutic agent; however, MIS is a large complex protein that has been difficult to generate in the large amounts that are necessary for clinical translation. In research studies, the delivery of MIS via a viral vector[7] and the use of antibodies specific for MISIIR that are able to mimic the
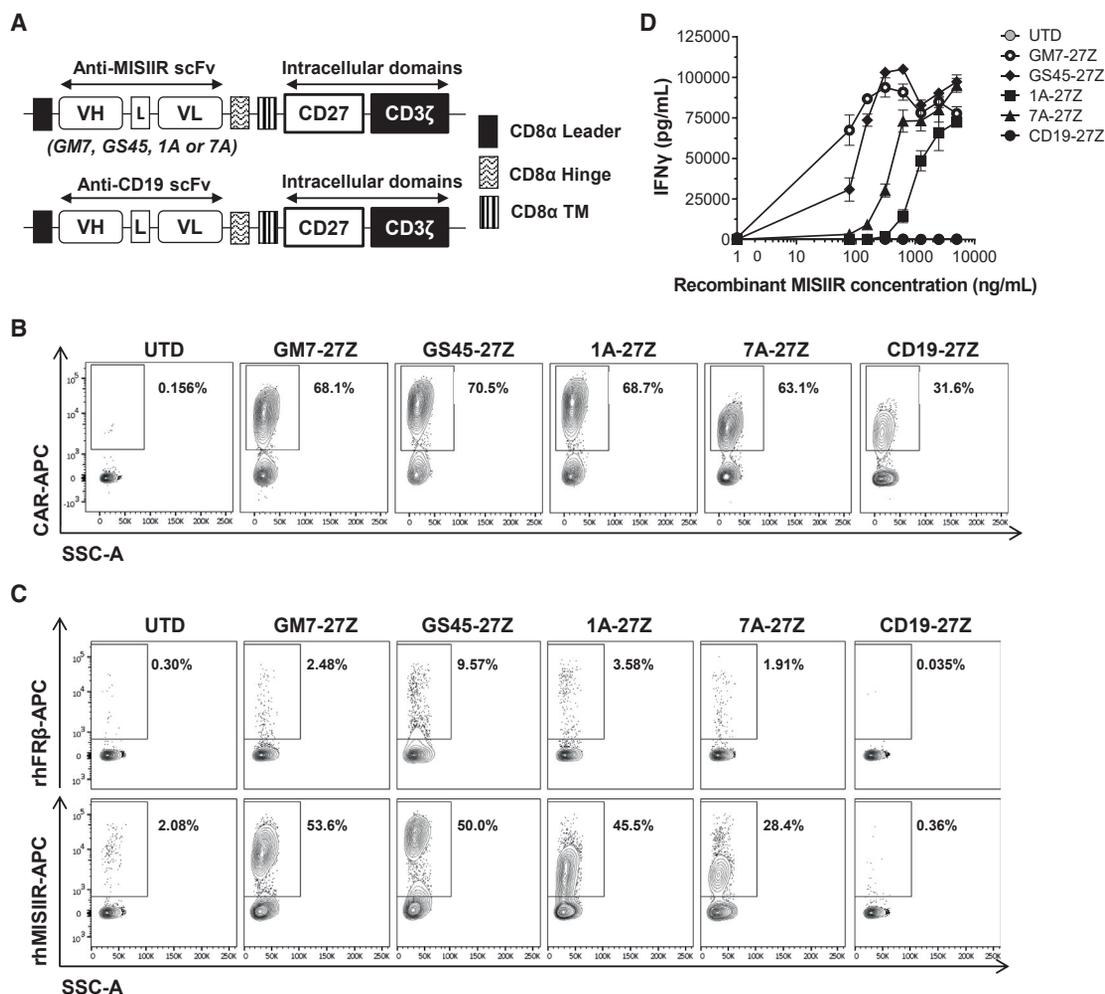
Figure 1. Generation of Anti-MISIIR CARs

(A) Schematic representation of lentiviral CAR expression vectors containing the anti-human MISIIR scFVs GM7, GS45, 1A, or 7A, or an anti-human CD19 scFv linked to the intracellular signaling domains from CD27 and CD3ζ in tandem. (B) Surface CAR expression in primary human T cells as detected by staining with a rabbit anti-human IgG (H+L) antibody. Results from a representative donor are shown. (C) CAR T cells were incubated in the presence of biotinylated recombinant human (rh)MISIIR or rhFRβ protein as control and stained with streptavidin-allophycocyanin (SA-APC) to detect antigen binding specificity. (D) IFN-γ as detected by ELISA in the supernatants of CAR T cells stimulated with immobilized rhMISIIR at increasing concentrations. Mean ± SD is represented. L, linker; TM, transmembrane domain; UTD, untransduced T cell; VH, variable heavy chain; VL, variable light chain. See also Figure S1.

natural effect of the ligand[16] are strategies reported to exploit the therapeutic value of the MIS/MISIIR pathway, but these agents have not yet advanced to clinical trials.

Herein, we propose an alternative approach of using MISIIR as a target for chimeric antigen receptor (CAR) T cell therapy to deliver specific and durable MISIIR targeting *in vivo*. The rationale is based in part upon the suggestion that MISIIR might be a natural target of tumor-infiltrating lymphocytes since MISIIR expression is associated with a better prognosis in OC patients whose tumors are highly infiltrated by CD3+ T cells.[17] Given the predicted potential and safety of MISIIR as an immunotherapy target, we sought to develop anti-MISIIR CAR T cell therapy for ovarian and endometrial cancer,

and to evaluate its efficacy and safety in different *in vitro* and *in vivo* preclinical models, including patient-derived (PD) tumor specimens.

RESULTS

Generation of Anti-MISIIR CARs

Anti-human MISIIR single-chain variable fragments (scFvs) were isolated from a human non-immune phage display library and characterized previously.[18,19] Four selected scFvs, namely GM7, GS45, 1A, and 7A, were cloned into validated lentiviral constructs containing a CD8α hinge and transmembrane domain with intracellular CD3ζ and CD27 signaling domains in tandem to create MISIIR-specific CARs.[20] Untransduced (UTD) and CAR T cells specific for human CD19 were used as controls in all experiments (Figure 1A). Human
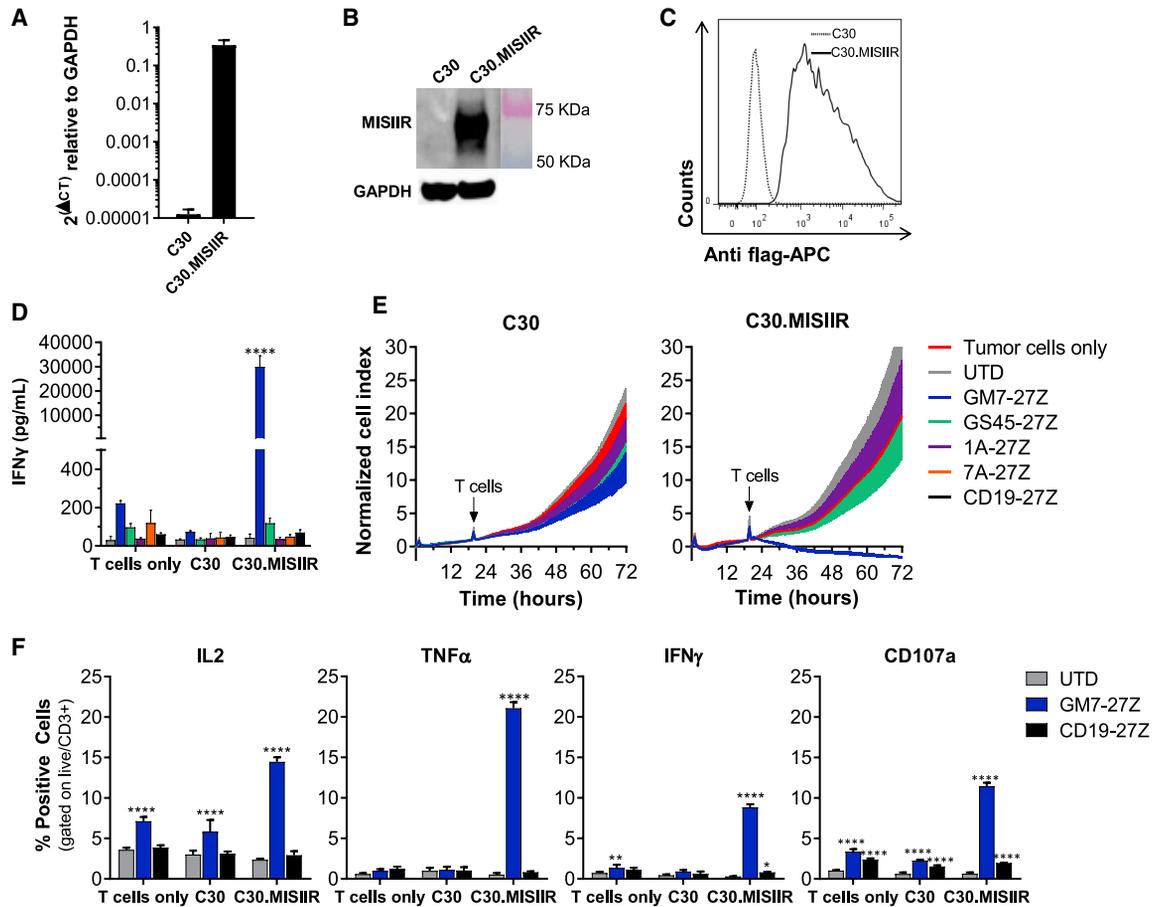
Figure 2. GM7 CAR T Cells Exhibit Antigen-Specific Reactivity Against Cell Surface MISIIR *In Vitro*

MISIIR-deficient OC cell line C30 was transduced to stably overexpress human MISIIR. (A–C) MISIIR expression on engineered C30.MISIIR was detected by (A) quantitative real-time PCR, (B) western blot analysis showing a predicted ~65-kb band, and (C) flow cytometry using an anti-flag antibody. For functional assays, co-cultures were performed at an E:T ratio of 1:1. (D) Antigen-specific IFN-γ production by MISIIR CAR T cells as detected by ELISA from 24-h co-culture supernatants. (E) Real-time cytotoxicity assays performed using xCELLigence technology in C30 and C30.MISIIR target cells. (F) Intracellular cytokine staining assay after 5 h of co-culture with target cells, showing IL-2, TNF-α, and IFN-γ production by GM7-27Z CAR T cells. Degranulation marker CD107a was also measured. Mean ± SD is represented for all experiments. Significance was determined by two-way ANOVA comparison and Tukey's multiple comparison test as compared to the UTD group. *$p < 0.05$, **$p < 0.01$, ****$p < 0.0001$. See also Figures S2 and S3.

T cells were transduced with the different CAR constructs at efficiencies that were reproducibly close to 70%. Transduction efficiencies were comparable between constructs as measured by surface CAR staining (Figure 1B). All constructs also demonstrated comparable cell doublings after 2 weeks of *in vitro* expansion (Figure S1A). After transduction and expansion, a CD4/CD8 T cell ratio of 30:70 was routinely achieved for all CAR constructs (Figure S1B).

Antigen specificity was assessed by incubating the T cells with biotinylated recombinant human MISIIR (rhMISIIR) or with a control protein (rhFRβ). All four MISIIR-specific CARs showed specific binding to rhMISIIR antigen, while no binding was observed when using the control protein or control UTD or CD19 CAR T cells (Figure 1C). T cells expressing any of the MISIIR-specific CAR constructs specifically secreted interferon (IFN)-γ upon stimulation with immo-

bilized rhMISIIR protein in a dose-response fashion (Figure 1D). GM7 and GS45 CAR constructs conferred the highest functional avidity to T cells, as demonstrated by their high cytokine release levels at low antigen density.

GM7 CAR T Cells Exhibit Antigen-Specific Reactivity against Cell Surface MISIIR

To test and compare the specific reactivity of the different CAR constructs against cell surface-expressed MISIIR, the human OC cell line C30, which lacks natural MISIIR surface expression, was engineered to constitutively express the target antigen (C30.MISIIR; Figures 2A–2C). After the various CAR T cells were co-cultured overnight with either parental C30 or C30.MISIIR, only GM7 and GS45 CAR T cells exhibited antigen-driven upregulation of the activation marker CD69 in response to C30.MISIIR but not C30 cells. 1A and 7A CARs
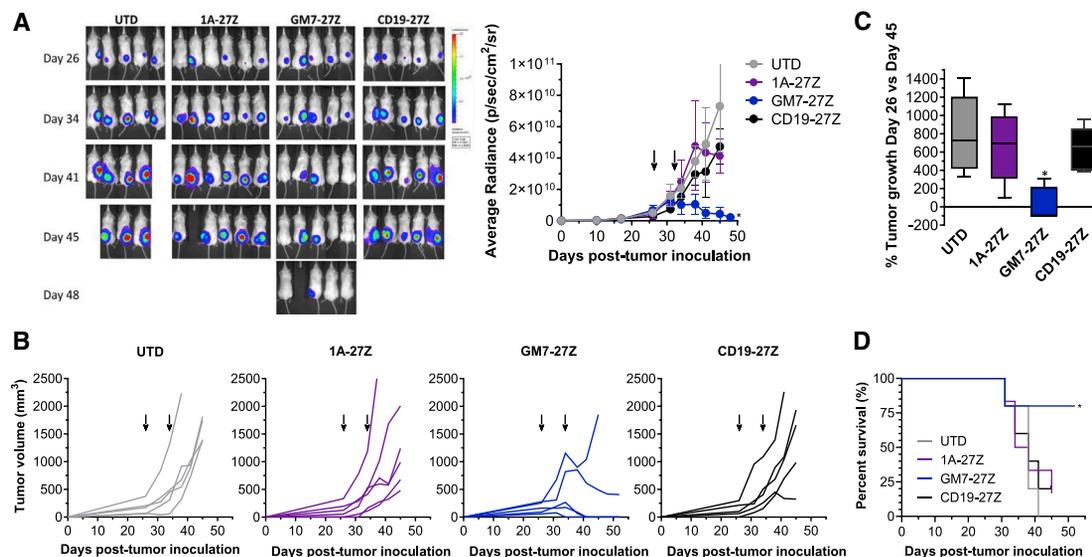
Figure 3. GM7 CAR T Cells Mediate Antitumor Activity *In Vivo*

C30.MISIIR GFP-fLuc cells (10×10^6) were inoculated into NSG mice subcutaneously. Once the tumors were established and reached a mean tumor volume of 150 mm³, mice were randomized in groups and CAR⁺ T cells (5×10^6) were given intravenously on days 26 and 33 post-tumor inoculation. (A and B) Tumor growth was monitored by (A) luminescence and (B) caliper measurement. (C) Representation of the percentage of tumor growth at day 45 versus day 26. Data are represented as mean ± SD of n = 5–6 mice per group. Significance was determined by one-way ANOVA with Tukey's multiple comparison test as compared to the UTD group. Arrows indicate time of CAR T cell administration. (D) Kaplan-Meier survival curves were plotted using a defined endpoint criterion of tumor volume equivalent to or greater than 1,000 mm³. Significance was determined by a log-rank Mantel-Cox test as compared to the UTD group. *p < 0.05.

did not confer reactivity (Figure S2). Supernatants from the same co-cultures were assayed for IFN-γ by ELISA, and they showed that only GM7 CAR T cells secreted high levels of IFN-γ in response to C30.MISIIR target cells (Figure 2D). Consistent with this result, GM7 was the only CAR capable of specifically lysing C30.MISIIR target cells while sparing parental C30 cells, as measured in a real-time cytotoxicity assay (Figure 2E). Despite showing antigen-specific binding and reactivity against rhMISIIR protein, GS45, 1A, nor 7A CAR displayed antigen-specific reactivity when the target was expressed on the surface of tumor cells. The possibility that the MISIIR epitopes recognized by these latter scFvs were not accessible by the CARs due to their relatively short hinges was considered. However, the replacement of the CD8α hinge by a longer immunoglobulin (Ig)G4-Fc-derived hinge (45 aa versus 228 aa long)[21] in the CAR constructs did not restore the reactivity of GS45, 1A, or 7A constructs, nor did it alter cytokine secretion levels by GM7 in co-culture with MISIIR-engineered C30 target cells (Figures S3A and S3B). Therefore, the GM7-27Z CD8α hinge was selected as the lead candidate anti-MISIIR CAR to advance.

Next, GM7 CAR (or control UTD and CD19 CAR) T cells were co-cultured for 5 h with C30 or C30.MISIIR cells, and production of the proinflammatory cytokines interleukin-2 (IL-2), tumor necrosis factor α (TNF-α) and IFN-γ was analyzed using intracellular cytokine staining. Degranulation, quantified by increased cell surface CD107a expression as a surrogate for T cell lytic function, was also assessed. A specific increase in each of these markers of CAR T cell response was observed solely in GM7 CAR T cells in the presence of C30.MISIIR (Figure 2F).

GM7 CAR T Cells Mediate Antitumor Activity *In Vivo*

Having observed that GM7 CAR T cells mediate responses against C30.MISIIR cells *in vitro*, their antitumor activity was investigated in a preclinical model. Non-obese diabetic (NOD)/severe combined immunodeficiency (SCID)/γ-chain⁻/⁻ (NSG) mice previously inoculated subcutaneously with C30.MISIIR cells were treated with UTD, CD19 CAR, non-reactive 1A anti-MISIIR CAR, or GM7 CAR T cells. Tumor progression was evaluated by luminescence (Figure 3A) and caliper measurements (Figures 3B and 3C). Mice receiving UTD or control CAR T cells showed clear evidence of tumor progression and eventually had to be euthanized due to large tumor burden. In contrast, treatment with GM7 CAR T cells completely eradicated tumors in three out of five treated mice, which remained clear of disease until the end of the experiment, 26 days after CAR T cell administration (tumors were not palpable and the bioluminescence signal was reduced to background levels from that time point forward), and controlled tumor progression in another mouse. Treatment with GM7 CAR T cells significantly prolonged survival as compared with mice from the control groups (Figure 3D). Signs of graft-versus-host disease (GVHD) were not observed at the endpoint of the *in vivo* study.

GM7 CAR T Cells Demonstrate Antigen-Specific Reactivity against Endogenous MISIIR

GM7 CAR T cell function was next evaluated against a panel of human tumor cell lines that express endogenous MISIIR at variable levels. Six different cell lines with previously reported MISIIR
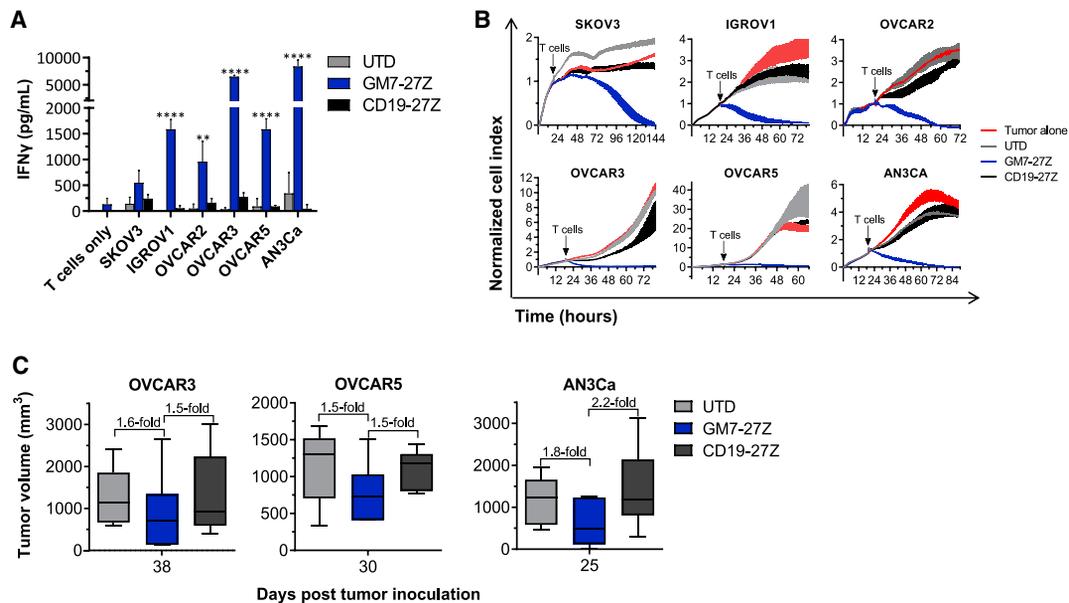
Figure 4. GM7 CAR T Cells Demonstrate Antigen-Specific Reactivity Against Endogenous MISIIR

(A) Antigen-specific IFN-γ production by MISIIR CAR T cells as detected by ELISA from 24-h co-culture supernatants. Co-cultures were established at a 1:1 E:T ratio. Significance was determined by two-way ANOVA and Dunnett's multiple comparison test as compared to the UTD group. **p < 0.01, ****p < 0.0001. (B) Real-time cytotoxicity assays established at a 3:1 E:T ratio. Data are represented as mean ± SD. (C) OVCAR3, OVCAR5, or AN3Ca GFP-fLuc cells were inoculated into NSG mice subcutaneously. Once the tumors were established, mice were randomized in groups and received two intravenous doses of CAR+ T cells (5 × 10^6) given 1 week apart. Tumor growth was monitored by caliper measurement. Means ± SD of tumor volumes at the endpoint of three individual in vivo studies are represented. See also Figure S6.

expression were assayed, including ovarian (IGROV1, SKOV3, OVCAR2, OVCAR3, and OVCAR5) and endometrial (AN3CA) cancer cell lines.[2–4,22] Immunohistochemistry (IHC) staining of tumor cell pellets confirmed MISIIR expression (Figure S4A). Surface MISIIR expression was also assessed by flow cytometry using multiple commercially available antibodies (Ab64762, PA5-13901, and AF4749) (Figure S4B). Only one of those antibodies, Ab64762 (Figure S4B, top panel), showed detectable surface levels of MISIIR at any level among the different cell lines.

After overnight co-culture of CAR T cells with target cells, supernatants were collected and assayed for IFN-γ by ELISA. GM7 CAR T cells secreted IFN-γ in response to target cells expressing endogenous MISIIR, while UTD or CD19 CAR T cells did not (Figure 4A). GM7 CAR T cells also specifically lysed all MISIIR-expressing cell targets (Figure 4B). At this point, the activity of GM7 CAR against cancer cell lines with natural MISIIR antigen expression was compared in the context of short CD8α or longer IgG4-Fc derived hinges, as well as CD27 or CD28 co-stimulatory domains. Higher levels of IFN-γ were secreted by the CAR containing the shorter hinge in co-culture with at least three out of the four MISIIR-expressing tumor cell lines tested (Figure S3C). Also, the CD28 co-stimulated CAR functioned specifically, albeit with reduced activity as compared to a CD27 CAR (Figure S5–S5C).

Antitumor efficacy in vivo was then tested in OVCAR3 and OVCAR5 OC xenograft models as well as in an AN3Ca endometrial cancer model. In all three tumor models, tumor growth was rapid and aggressive. Nevertheless, tumors from mice treated with GM7 CAR T cells were 1.5-fold smaller than tumors in UTD and CD19 CAR control-treated groups at the study endpoint in OVCAR3 and OVCAR5 models. In the AN3Ca model, tumor volume was 1.8- and 2.2-fold lower in GM7-treated mice at the end of the experiment, compared to UTD and CD19 CAR-treated groups, respectively (Figure 4C; Figure S6A). In addition, in the AN3Ca tumor model, higher concentrations of circulating CD3+ T cells were detected 18 days after T cell administration in mice treated with GM7 CAR as compared to mice from the UTD group (Figure S6B), as well as a trend to higher frequencies of CD45+ cells infiltrating the tumors at the endpoint of the experiment (Figure S6C).

The Killing Mechanism of GM7 CAR T Cells Does Not Involve Ligand-Induced Apoptosis

The natural ligand for MISIIR, MIS, triggers cancer cell apoptosis by engaging MISIIR;[2,12] however, producing large quantities of rhMIS protein for the treatment of patients has been challenging. Alternatively, MISIIR-specific antibodies that induce apoptosis upon receptor engagement have been previously reported.[16] To test the hypothesis that anti-MISIIR CARs can trigger cancer cell apoptosis in a manner analogous to MIS, a signaling-deficient CAR, GM7-Δζ, that is able to bind to MISIIR through the extracellular scFv domain but is incapable of signaling through the T cell intracellular domains to initiate T cell activation was created (Figure 5A). GM7-Δζ was detected on the cell surface at similar levels than GM7-27Z,
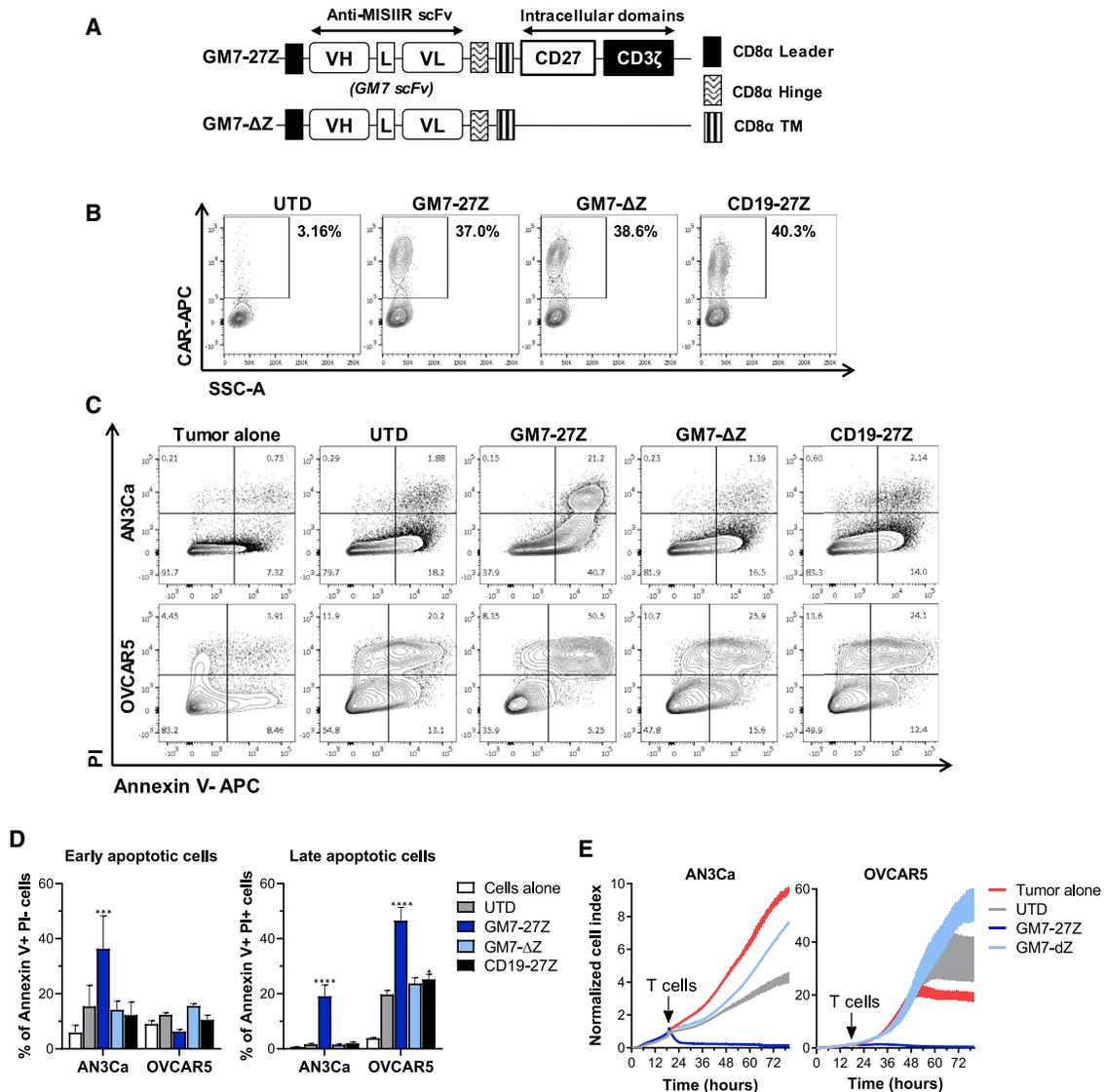
Figure 5. The Killing Mechanism of GM7 CAR T Cells Does Not Involve Ligand-Induced Apoptosis

(A) Schematic representation of the delta ζ (Δζ) CAR construct. (B) Surface CAR expression in primary human T cells as detected by staining with a rabbit anti-human IgG (H+L) antibody. (C) Representative flow plots of the staining of apoptotic markers annexin V (x axis) and PI (y axis) after 48 h of co-culture at a 3:1 E:T ratio. GFP$^+$ tumor cells were gated prior to analysis of apoptotic markers. (D) Frequency of early (annexin V$^+$ PI$^-$) and late (annexin V$^+$ PI$^+$) apoptotic cells. Significance was determined by two-way ANOVA and Dunnett's multiple comparison test as compared to the UTD group. *$p < 0.05$, ****$p < 0.0001$. (E) Real-time cytotoxicity assays established at a 3:1 E:T ratio. Data are represented as mean ± SD. See also Figure S7.

demonstrating that deleting CD27-CD3 domains did not impact surface expression of the CAR (Figure 5B). AN3Ca or OVCAR5 cells, which are MIS responsive, were co-cultured with GM7 CAR T cells or its signaling-deficient Δζ counterpart and evaluated for induction of apoptosis. In spite of the capacity of GM7 scFv to bind to MISIIR, the GM7-Δζ CAR was unable to trigger apoptosis in MISIIR-expressing target cells (Figures 5C and 5D). Real-time cytotoxicity assays (Figure 5E) and MTS cell proliferation assays (data not shown) confirmed that constructs that contain only the extracellular part of the CAR without intracellular signaling capacity were not able to

inhibit tumor growth in an activation-independent manner. Similar results were observed using IGROV1 targets cells (Figures S7D–S7F), which are also MIS responsive, or in the engineered model C30.MISIIR (Figures S7A–S7C). These data indicate that MISIIR CAR-mediated killing of cancer cells is highly dependent on CAR T cell activation.

GM7 CAR T Cells Show Reactivity in PD Tumor Specimens

As a route toward future clinical application, GM7 CAR T cells were tested against PD tumor specimens *in vitro*. Samples from two
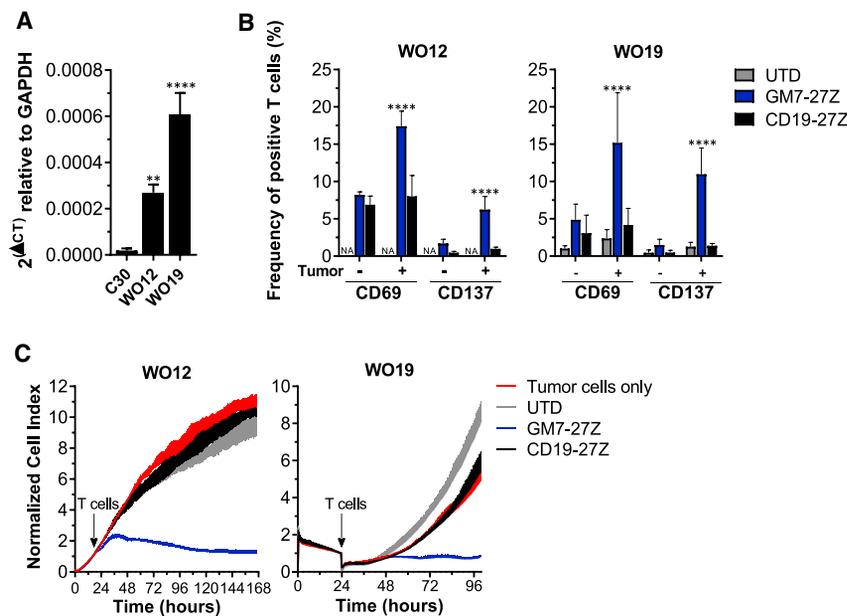
Figure 6. GM7 CAR T Cells Show Reactivity in Patient-Derived Tumor Specimens

(A) MISIIR expression in patient-derived tumors as detected by quantitative real-time PCR. Significance was determined by one-way ANOVA comparison and Dunnett's multiple comparison test. **$p < 0.01$, ****$p < 0.0001$. WO12 or WO19 cell cultures were co-cultured for 24 h with T cells at a 1:1 E:T ratio. (B) Frequency of live/CD3+ cells expressing the T cell activation markers CD69 and CD137 were quantified by flow cytometry staining. Data are represented as mean ± SD. Significance was determined by two-way ANOVA and Tukey's multiple comparison test. ***$p < 0.001$, ****$p < 0.0001$ as compared to all of the other groups. (C) Real-time cytotoxicity assays established at a 3:1 E:T ratio.

different high-grade serous OC (HGSOC) PD tumors (WO12 and WO19) were obtained and confirmed for positive human MISIIR mRNA expression by quantitative real-time PCR, as compared to the negative cell line C30 (Figure 6A). WO12 or WO19 tumor cells were co-cultured overnight alone or with GM7 CAR, control CD19 CAR, or UTD T cells. T cells were then assessed for the expression of CD69 and CD137 (4-1BB) T cell activation markers. Significant antigen-driven upregulation of both activation markers was observed in GM7 CAR, but not control, T cells when co-cultured with either WO12 or WO19 tumor cells (Figure 6B). GM7 CAR T cells also demonstrated antigen-specific antitumor activity against WO12 and WO19 cells in real-time cytotoxicity assays (Figure 6C).

GM7 CAR T Cells Do Not Mediate Detectable On-Target Off-Tumor Toxicity

Despite the restricted expression profile of MISIIR in normal tissues, on-target off-tumor toxicity is a key factor to be considered when developing novel CAR T therapies. To begin to address this concern, GM7 or CD19 CAR T cells were co-cultured at different effector-to-target (E:T) ratios with a panel of primary human normal cell lines derived from aortic and pulmonary myocytes, small airway and renal epithelial cells, neuronal progenitors, and keratinocytes, and chromium release cytotoxicity assays were performed. Selection of these cell types was based on reported low levels of MISIIR protein expression in the literature as well as cell availability.[4,23] A CAR specific for SSEA4, named MC813-70, which demonstrates normal tissue toxicity, was used as a positive control for normal cell targeting.[24] Similar to CD19 CAR T cells, whose on-target off-tumor toxicity is limited only to CD19+ normal B cells in patients, GM7 CAR T cells showed no reactivity against this limited panel of normal human primary cells, except for low level lysis of aortic smooth myocytes that was only observed at the highest E:T ratio tested (10:1). Importantly,

no killing was observed for the same cell type obtained from pulmonary artery. GM7 CAR T cells did lyse positive control C30.MISIIR cells. In contrast, MC813-70 CAR T cells lysed all target cells tested (Figure 7). While these studies are limited, as not all human tissues are represented, they serve as an initial screen for off-tumor activity. We next evaluated the potential for toxicity in the various preclinical xenograft models. These studies bear significance since the GM7 CAR is cross-reactive with the mouse MISIIR homolog, resulting in mMISIIR-specific T cell release of IFN-γ (Figure S8A) as well as mMISIIR-specific tumor cell lysis in vitro (Figure S8B) of the mouse OC cell line ID8, which expresses mMISIIR.[25] In all of the preclinical studies performed, there was no overt evidence of toxicity associated with the administration of GM7 CAR T cells to mice, as measured by body weight loss and physical signs of toxicity (data not shown).

DISCUSSION

Herein, we described a CAR designed to target human MISIIR for the treatment of gynecologic cancers. MISIIR is expressed at high levels in OC and also in endometrial cancer, a disease for which novel therapeutic strategies are more limited and in need.[4] Moreover, many articles described expression of MISIIR in cervical, breast, prostate, and lung cancer, and ocular melanoma, broadening the potential applicability of this form of therapy.[6,8,10,11]

CAR T cells have shown dramatic clinical success for the treatment of hematologic malignancies.[26] The facts that (1) OC patients whose tumors are infiltrated by T cells have better overall survival,[27] and (2) ovarian tumors express targetable tumor-associated antigens on their surface provide the rationale for developing CAR T cell therapies in this disease. In gene-engineered T cell trials for OC that target antigens such as FRα, NY-ESO-1, Her2, MSLN, or MUC16, T cell therapy has yet to recapitulate the success of CD19 CAR T cell therapy in cancers of the blood.[28] One challenge to designing effective CAR T cell therapy for solid tumors is the selection of an appropriate target antigen that is selectively, highly, and homogeneously expressed in tumor cells. Given the established
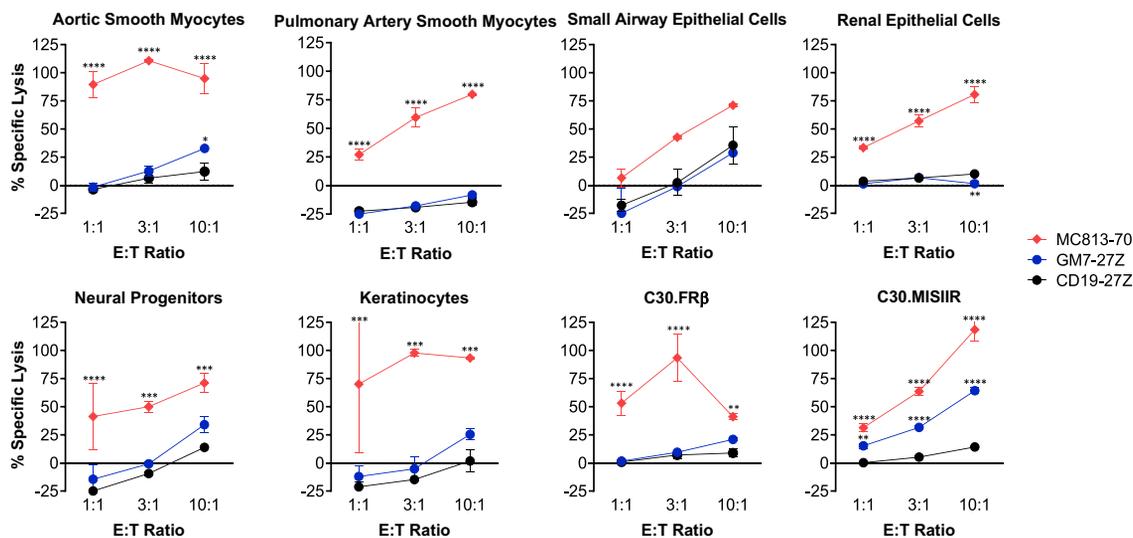
Figure 7. GM7 CAR T Cells Do Not Mediate Detectable On-target Off-tumor Toxicity

GM7-27Z and CD19 CAR T cells were tested in 16-h chromium-release lysis assays at E:T ratios of 1:1 to 10:1. MC813-70 CAR T cells, known to exhibit normal tissue toxicity, were used as a positive control. In addition, the various CAR T cells were tested on C30 or C30.MISIIR tumor cell lines. Data are represented as mean ± SD. Statistical comparisons were determined by two-way ANOVA and Dunnett's multiple comparison test as compared to CD19 CAR. **p < 0.01, ***p < 0.001, ****p < 0.0001.

relevance of the MIS/MISIIR pathway in cancer,[29] as well as the challenges associated with the large-scale production of rhMIS protein for therapeutic use, we developed a different strategy of targeting MISIIR using a CAR T cell approach.

In our study, all of the CAR constructs generated are based on fully human scFvs, avoiding potential issues related to transgene immunogenicity.[30,31] While all of these MISIIR CARs conferred T cells with the ability to recognize rhMISIIR protein, only one CAR construct, namely GM7, was capable of redirecting T cell activity against MISIIR expressed on the cell surface. The reason for which the rest of the CAR constructs did not show reactivity against C30.MISIIR target cells remains unclear, although it does not appear to be related to CAR expression, affinity of the scFv for the target, or overall targeting, as MISIIR is expressed at very high levels in the engineered cell line. In an extensive set of *in vitro* assays, GM7 CAR T cells specifically and reproducibly recognized MISIIR-expressing ovarian and endometrial cancer cells, produced multiple pro-inflammatory cytokines, and mediated cancer cell cytolysis.

Although CD28 or 4-1BB co-stimulated CAR constructs are already validated in patients and CD19 CAR T cells based on both co-stimulatory domains have been US Food and Drug Administration (FDA) approved recently, the CD27 co-stimulation domain was used in our constructs. CD27 belongs to the same family as 4-1BB, and very similar features have been observed between them in the context of an anti-FRα CAR.[32] Both CD28 and CD27 moieties were directly compared in the context of GM7 CAR, with CD28 showing a slower killing kinetics *in vitro* as well as lower levels of IFN-γ secretion when co-cultured with any one of four different tumor cell lines (IGROV1,

OVCAR3, OVCAR5, and AN3Ca) as compared to the CD27 counterpart (Figure S5).

In an earlier study, one antibody specific for MISIIR, 12G4, was reported to induce apoptosis in MISIIR-expressing tumor cell lines,[33] prompting us to hypothesize that CAR T cells might have a similar effect and induce tumor cell death by dual mechanisms of MISIIR receptor engagement as well as by T cell-mediated cytotoxicity. This hypothesis was not supported by the finding that the GM7-Δζ CAR, which engages MISIIR protein but lacks intracellular T cell activation potential, was unable to induce cancer cell apoptosis. The fact that 12G4 antibody and MIS protein bind to non-overlapping epitopes on MISIIR implies that receptor internalization may be critical to activate the signaling and degradation pathways, as opposed to a surface ligand-mimicking binding effect.[16] In future studies, it may be beneficial to screen MISIIR scFvs for their ability to bind to the MIS-binding epitope or to induce apoptosis of target cells, prior to the generation and screening of new CARs.

In spite of its inability of induce apoptosis, the GM7 CAR allowed T cells to effectively lyse a range of tumor cell lines expressing variable surface levels of the MISIIR target antigen. A particularly relevant model used in this study was the PD tumor specimens. The possibility of establishing primary cell cultures from PD tumors is of great value to directly test therapeutic strategies for individual patients in a relatively rapid manner. In a study by Pépin et al.,[7] MISIIR protein expression was detected in 16 PD tumor cell lines. Regardless of the limited number of samples utilized in our study, the two tumors tested expressed significant levels of MISIIR as compared to a negative tumor cell line. GM7 CAR T cells specifically recognized and reacted

in co-culture with both MISIIR-expressing PD tumor samples, WO12 and WO19, demonstrating the potential of the treatment of OC patients with this CAR approach.

Using the high ectopic MISIIR-expressing C30.MISIIR xenograft model, complete tumor eradication was observed in three of five treated mice, with tumor outgrowth ultimately occurring in the other two mice. In the case of other aggressive xenograft models, where MISIIR is naturally expressed at more moderate levels, the *in vivo* efficacy of GM7 CAR T cells was modest. When MISIIR expression on the remaining tumor was assessed by qPCR, lower, albeit non-significant, levels were detected, as compared to tumors from mice treated with control UTD or unspecific CD19 CAR T cells, suggesting that antigen downregulation or loss might be occurring as a means of escape (data not shown). Beyond antigen loss and lower expression levels of surface target, heterogeneous expression of MISIIR in tumors might limit efficacy. In one study looking at OC patient specimens, expression percentages in MISIIR-expressing cases ranged between 20% and 95%, suggesting that MISIIR heterogeneous expression may exist in patients.[33] Another study also found variable levels of MISIIR expression in different tumor cores from the same patient, with some cores that were negative for MISIIR staining within the same cases.[7] Combinatorial targeting of multiple antigens co-expressed in OC might be needed to overcome this issue. This strategy is being tested clinically in the case of CD19 loss in relapsed patients treated with CD19 CAR T cells by additionally targeting the antigen CD22.[34]

High levels of MISIIR expression in adults is confined to granulosa cells in the ovary, as well as Sertoli and Leydig cells in the testis.[35] In the largest study of MISIIR expression in gynecologic tumors and benign tissue reported to date, MISIIR protein was detected in 28% of the tested normal endometrium samples (versus 75% of endometrial cancer specimens), fallopian tube, and placenta in women.[4] Weak IHC staining of MISIIR was also revealed in selected normal non-gynecologic tissues such as liver parenchyma, bronchiolar epithelium, small intestine mucosa, kidney, adrenal, pancreas, and breast ducts, and at lower levels in tonsil, lymph nodes, and arterial smooth muscle. Importantly, 74% of human normal tissues evaluated did not express MISIIR protein.[4]

We evaluated the activity of GM7 CAR T cells *in vitro* against a normal cell panel that included cells from some of the tissues reported to express MISIIR protein, such as renal epithelial cells, small airway epithelial cells, or artery smooth myocytes.[4] Neural progenitors were also included, as expression of MISIIR mRNA and protein in motor neurons has been reported in mice (although not in humans).[23] In general, GM7 CAR T cells did not recognize normal cells. However, a very low level of aortic smooth myocyte lysis was observed and only at the highest E:T ratio tested, but lysis of smooth myocytes obtained from the pulmonary artery was not detected. Whether this *in vitro* finding represents an experimental artifact is unclear, yet these results bear consideration when translating to the clinical setting. It is notable that many noncoding transcripts and alternative splice isoforms of MISIIR have been identified, some of which are retained in the endoplasmic reticulum (ER) and not expressed on the cell surface, making them unlikely targets for CAR T cells.[36–39] In our preclinical models, physical signs of GM7 CAR-associated toxicity were not observed in any experiment conducted, in spite of the established reactivity of the GM7 CAR against both human and mouse MISIIR protein homologs. In line with our observations, Sakalar et al.[25] targeted MISIIR by utilizing a DNA vaccine in the mouse OC model ID8 and showed an induction of tumor immunity by the vaccine in the absence of any severe autoimmune consequences. Even if MISIIR is expressed in normal tissue, the level of MISIIR found in normal tissues has been reproducibly shown to be significantly lower than in malignant cells.[4,39] In this setting, tuning the affinity and functional avidity of the CAR construct expressed in T cells may serve as a strategy to overcome any potential toxicity issues.[40] Furthermore, the expression of higher levels of MISIIR in healthy gynecologic tissues is also manageable, as these reproductive tissues are not essential for sustaining the life of the patient, and some of which are commonly removed by surgical resection in advanced OC patients.

Herein, we report a MISIIR targeting strategy that relies on the use of CAR T cell technology. This alternative approach to MISIIR targeting overcomes the issues in generating sufficient quantities of rhMIS protein as a therapeutic agent and is backed by the effector functions of a T cell in order to deliver MISIIR-specific cytotoxicity. Taken together, the data presented herein serve as the foundation for the clinical development of MISIIR-specific CAR T cell therapy for the safe and efficacious treatment of MISIIR-expressing OC and other malignancies.

MATERIALS AND METHODS
Cells
All cells were cultured at 37°C in complete media (CM, RPMI 1640 GlutaMAX, 10% fetal bovine serum, 100 U/mL penicillin, 100 μg/mL streptomycin) and regularly validated to be mycoplasma free. Lentivirus packaging was performed in the immortalized normal fetal renal 293T cell line purchased from ATCC. Ovarian carcinoma cell line C30 was provided by George Coukos (Ludwig Institute for Cancer Research, Lausanne, Switzerland).[41] C30 was transduced with a lentiviral vector encoding human MISIIR cDNA (Origene, catalog no. RC212425) to generate C30.MISIIR. IGROV1 and OVCAR5 were kindly provided by Ronny Drapkin (Ovarian Cancer Research Center, University of Pennsylvania, Philadelphia, PA, USA). OVCAR3 and SKOV3 were a gift from Carl June (Center for Cellular Immunotherapies, University of Pennsylvania, Philadelphia, PA, USA). AN3Ca was purchased from the ATCC. All of the cell lines were stably transduced with GFP-2A-firefly luciferase (fLuc) lentiviral vector. Normal human cells were provided by Laura Johnson (neural progenitors were obtained from Aruna Bio, and the rest of the cells were from PromoCell). WO19 primary tumor cultures were established from tumor obtained from patients after being passaged in mice in order to expand the tumor as described.[42] WO12 primary tumor cultures were established from tumor obtained from patients at the time of OC debulking surgeries as previously described.[43] Primary

tumor cells were grown on Primaria tissue culture flasks (Corning) in hypoxic conditions until required for *in vitro* experiments.

Anti-MISIIR CAR Construction

Plasmids encoding for GM7, GS45, 1A, and 7A scFvs were obtained from Gregory Adams (Fox Chase Cancer Center, Philadelphia, PA, USA).[18,19] All scFvs were polymerase chain reaction (PCR) amplified using the following paired primers: 5′-TAT<u>GGATCC</u>GCC CAGGTGCAGCTGGTGCAGTCTGGAAC-3′ (<u>BamHI</u>) and 5′-TAT <u>GCTAGC</u>CGAGGGGGCGGCCTTGGGCTGACCTAG-3′ (<u>NheI</u>); 5′-TAT<u>GGATCC</u>GCCCAGGTGCAGCTGGTGGAGTCTGGG-3′ (<u>BamHI</u>) and 5′-TAT<u>GCTAGC</u>ACGTTTGATCTCCAGCTTGG TCCCTCCGC-3′ (<u>NheI</u>); 5′-TAT<u>TGATCA</u>GCCGAGGTGCAGCT GGTGCAGTCTGGG-3′ (<u>BclI</u>) and 5′-TAT<u>GCTAGC</u>CGAGTGGG CAGCCTTGGGCTGACCGAG-3′ (<u>NheI</u>); 5′-TAT<u>GGATCC</u>GCC GAGGTGCAGCTGGTGGAGTCTG<u>GG</u>-3′ (<u>BamHI</u>) and 5′-TAT <u>GCTAGC</u>CGAGGGGGCAGCCTTGGGCTGACCTAGG-3′ (<u>NheI</u>). The PCR product was digested and ligated into previously described third-generation pELNS lentiviral vectors containing CD27-CD3Z signaling domains.[32] The resulting constructs were designated pELNS-GM7-27Z, pELNS-GS45-27Z, pELNS-1A-27Z, and pELNS-7A-27Z. pELNS-CD19-27Z was also previously described.[32] A pELNS-GM7-ΔZ construct, lacking the signaling domains but maintaining the extracellular scFv portion, the transmembrane domain, and a non-functional 5-aa-long intracellular tail, was generated as reported previously.[32] Lentiviral vectors were produced in 293T cells as previously described.[44]

Generation of CAR T Cells

Primary lymphocytes from normal donors were obtained from the University of Pennsylvania Human Immunology Core. T cells were stimulated, transduced, and expanded as previously described.[44] Briefly, CD4 and CD8 T cells were mixed at 1:1 ratio and activated with CD3/CD28 Dynabeads (Invitrogen, Carlsbad, CA, USA) at a bead-to-cell ratio of 3:1. 24 h after activation, T cells were transduced with lentiviral vectors at an MOI of 10 and expanded in CM with 50 IU/mL human IL-2 (Proleukin, Prometheus Laboratories, San Diego, CA, USA) for 10–14 days. Cell size was monitored using a Multisizer-3 Coulter Counter (Beckman Coulter, Brea, CA, USA). Rested T cells (<300 fL) were cryopreserved or used for functional *in vitro* and *in vivo* assays.

Flow Cytometric Analysis

All samples for flow cytometry were labeled in 100 μL of staining buffer (phosphate-buffered saline, 2% fetal bovine serum) at 4°C. In all analyses, singlets were gated on using forward scatter height (FSC-H) versus forward scatter area (FSC-A), followed by gating based on forward versus side scatter characteristics. All experiments were conducted on a BD LSRFortessa flow cytometer (Becton Dickinson, Franklin Lakes, NJ, USA) and analyzed with FlowJo v10 (BD Biosciences, Franklin Lakes, NJ, USA). For all experiments, T cell suspensions were stained with fixable Live/Dead aqua stain (Invitrogen), followed by surface antibody staining. Expression of CAR proteins was detected using biotinylated rabbit anti-human IgG (H+L)

(Jackson ImmunoResearch, West Grove, PA, USA; catalog no. 309-065-003), biotinylated recombinant MISIIR, or recombinant control protein FRβ (R&D Systems, Minneapolis, MN, USA), followed by streptavidin-allophycocyanin (APC) (BD Biosciences, Franklin Lakes, NJ, USA; catalog no. 554067). Expression of MISIIR in engineered C30.MISIIR cells was assessed by anti-DYKDDDDK-APC (Miltenyi Biotec, Bergisch Gladbach, Germany; catalog no. 130-101-564). The following antibodies against human molecules were used: anti-CD3-Brilliant Violet (BV)605 (catalog no. 317321), anti-CD3-peridinin chlorophyll protein (PerCP)/Cy5.5 (catalog no. 300327), anti-CD4-fluorescein isothiocyanate (FITC) (catalog no. 317408), anti-CD4-BV421 (catalog no. 317433), anti-CD8-APC (catalog no. 300911), anti-CD69-Pacific Blue (catalog no. 310919), anti-CD137-phycoerythrin (PE)/Cy7 (catalog no. 309817), and anti-TNF-α−BV650 (catalog no. 502928) from BioLegend (San Diego, CA, USA); anti-CD107a-Alexa Fluor 700 (Alexa700) (catalog no. 561340) and anti-CD8-APC-H7 (catalog no. 561423) from BD Biosciences (Franklin Lakes, NJ, USA); and anti-CD45-PE (catalog no. 12-9459-42), anti-IFN-γ-PE (catalog no. 12-7319-42), and anti-IL-2-PerCP-eFluor 710 (catalog no. 46-7029-42) from eBioscience (Waltham, MA, USA).

In Vitro Co-culture Experiments

Cytokine release assays were performed by co-culture of 1×10^5 T cells with either soluble recombinant MISIIR protein (kindly provided by Gregory Adams, Fox Chase Cancer Center, Philadelphia, PA, USA) at increasing concentrations, or 1×10^5 target cells per well in triplicate in 96-well plates in a final volume of 200 μL of CM. After 24 h, co-culture supernatants were assayed for the presence of IFN-γ using an ELISA kit, according to the manufacturer's instructions (BioLegend, San Diego, CA, USA). From the same co-cultures, T cells were collected and stained for T cell markers CD3, CD4, and CD8, as well as surface activation markers CD69 and CD137. For apoptosis assays, tumor cells were co-stained with annexin V-APC and propidium iodide (PI) (BioLegend, San Diego, CA, USA; catalog no. 640912), according to the manufacturer's instructions. For intracellular staining, 1×10^5 CAR T cells were co-cultured with target cells at 1:1 E:T ratio in triplicate in 200 μL of CM in the presence of anti-CD107a antibody and GolgiStop protein transport inhibitor (BD Biosciences, San Diego, CA, USA). After 5 h, cells were stained with Live/Dead, followed by surface markers CD3, CD4 and CD8, and then fixed and permeabilized by using the Cytofix/Cytoperm fixation/permeabilization kit (BD Biosciences, San Diego, CA, USA; catalog no. 554715) according to the manufacturer's instructions. Finally, cells were stained for intracellular cytokines IFN-γ, TNF-α, and IL-2.

Cytotoxicity Assays

Cytotoxic killing of target tumor cells was assessed using the xCELLigence real-time cell analyzer system (ACEA Biosciences, San Diego, CA, USA). Target tumor cells were plated at 1×10^4 cells/well in 96-well plates. After overnight cell adherence, T cells were added at the indicated E:T ratios. Cell index (relative cell impedance) was monitored every 20 min and normalized to the maximum cell index

value immediately prior to effector-cell plating. Shaded lines reflect the mean of triplicate wells ± SD. Cytotoxicity of CAR T cells cultured with normal human primary cells was evaluated in a ^{51}Cr-release assay. 1×10^6 target cells were labeled with ^{51}Cr (50 mCi) for 1 h at 37°C. 1×10^4 labeled target cells were plated in each well of a 96-well plate, and effector cells were added in a volume of 100 μL at the indicated E:T ratios. Cells were co-incubated for 16 h at 37°C, and 30 μL of supernatant was collected and transferred onto the filter of a LumaPlate (PerkinElmer, Waltham, MA, USA). Radioactivity on dried LumaPlate was measured using a β-emission-reading liquid scintillation counter. Percentage specific lysis was determined using the reading of target cells alone and Triton X-100-lysed target cells, corresponding to 0% lysis and 100% lysis, respectively.

Gene-Expression Analysis by RT-PCR

Quantitative real-time PCR was used to analyze expression of MISIIR. RNA from frozen cell pellets or tumor samples was extracted with an RNeasy Mini kit (QIAGEN, Hilden, Germany) and reverse transcribed with a high-capacity RNA-to-cDNA kit (Applied Biosystems, Waltham, MA, USA), according to the manufacturer's instructions. Quantitative real-time PCR was performed using TaqMan Universal PCR Master Mix in a ViiA 7 real-time PCR system. The following probes were purchased from Applied Biosystems: AMHR2 (Hs01086646_g1) and glyceraldehyde-3-phosphate dehydrogenase (GAPDH) (Hs02786624_g1). Target gene expression was calculated by the $2^{-\Delta\Delta CT}$ method for relative quantification after normalization to GAPDH expression.

Xenograft Models

The University of Pennsylvania Institutional Animal Care and Use Committee (IACUC) approved all animal experiments. NSG mice were purchased from The Jackson Laboratory and bred and housed in the vivarium at the University of Pennsylvania in pathogen-free conditions. Xenograft tumors were established by subcutaneous injection of 10×10^6 C30.MISIIR, 4×10^6 OVCAR3, and 1×10^6 OVCAR5 or AN3Ca into the flanks of NSG mice. At indicated days, mice were treated with two intravenous injections of 5×10^6 CAR$^+$ T cells on days 0 and 7. Tumors were measured twice a week with caliper, and volumes were calculated as V = 1/2 × Length (L) × Width (W) × W. Mice were euthanized when tumor diameter was equivalent to or greater than 2 cm. Bioluminescence imaging was performed by using a Lumina IVIS imaging system and quantified with the Living Image software (PerkinElmer, Waltham, MA, USA). Mice were given an intraperitoneal injection of 150 mg/kg D-luciferin (Caliper Life Sciences, Hopkinton, MA, USA) and imaged under isoflurane anesthesia at the peak of photon emission.

Western Blot

Cells were lysed using radioimmunoprecipitation assay (RIPA) lysis buffer containing protease inhibitor cocktail (Roche, Basel, Switzerland; catalog no. 5892970001). Protein was quantified using a bicinchoninic acid (BCA) assay (Thermo Scientific, Waltham, MA, USA; catalog no. 23227). 80 μg of protein samples was mixed with Laemmli loading buffer (Bio-Rad, Hercules, CA, USA; catalog no. 161-0737) and 5% β-mercaptoethanol (Bio-Rad, Hercules, CA, USA; catalog no. 60-24-2) and incubated at 95°C for 5 min. Lysates were loaded in 4%–15% Mini-PROTEAN TGX gels (Bio-Rad, Hercules, CA, USA; catalog no. 456-1033), and gels were run at 150 V for 1 h. A protein ladder (Bio-Rad, Hercules, CA, USA; catalog no. 161-0376) was used. Protein samples were then transferred from gels to a polyvinylidene fluoride (PVDF) membrane (Millipore, Burlington, MA, USA; catalog no. IPVH00010) at 100 V for 1 h. Membranes were blocked and washed with Tris-buffered saline with Tween 20 (TBST) (1% Tween 20) (Bio-Rad, Hercules, CA, USA; catalog no. 170-6435) and incubated with primary human MISIIR antibody (R&D Systems, Minneapolis, MN, USA; catalog no. AF4749) at 0.1 μg/mL and secondary antibody peroxidase-conjugated AffiniPure donkey anti-sheep IgG (H+L) (Jackson ImmunoResearch, West Grove, PA, USA; catalog no. 713-035-147) diluted 1:10,000. Human/mouse/rat GAPDH (R&D Systems, Minneapolis, MN, USA; catalog no. MAB5719) diluted 1:20,000 was used as housekeeping control. Membranes were washed three times in between the primary and secondary antibodies incubation steps. Consequently, membranes were developed using the enhanced chemiluminescence (ECL) prime western blotting detection reagent (GE Healthcare, Chicago, IL, USA; catalog no. RPN2236) and imaged using a GE ImageQuant LAS 4000 series imaging system.

Statistical Analysis

The data are reported as mean ± standard deviation (SD) unless otherwise noted. Statistical analysis was performed using one-way ANOVA, two-way ANOVA with a Tukey's or Dunnett's multiple comparisons *post hoc* test, or unpaired Student's t test when appropriate. *In vitro* assays were replicated with at least three different normal T cell donors. GraphPad Prism 8.0 software (La Jolla, CA, USA) was used for statistical calculations. $p < 0.05$ was considered significant.

SUPPLEMENTAL INFORMATION

Supplemental Information can be found online at https://doi.org/10.1016/j.ymthe.2019.11.028.

AUTHOR CONTRIBUTIONS

CONFLICTS OF INTEREST

REFERENCES

1. Teixeira, J., Maheswaran, S., and Donahoe, P.K. (2001). Müllerian inhibiting substance: an instructive developmental hormone with diagnostic and possible therapeutic applications. Endocr. Rev. 22, 657–674.

2. Masiakos, P.T., MacLaughlin, D.T., Maheswaran, S., Teixeira, J., Fuller, A.F., Jr., Shah, P.C., Kehas, D.J., Kenneally, M.K., Dombkowski, D.M., Ha, T.U., et al. (1999). Human ovarian cancer, cell lines, and primary ascites cells express the human Mullerian inhibiting substance (MIS) type II receptor, bind, and are responsive to MIS. Clin. Cancer Res. 5, 3488–3499.

3. Renaud, E.J., MacLaughlin, D.T., Oliva, E., Rueda, B.R., and Donahoe, P.K. (2005). Endometrial cancer is a receptor-mediated target for Mullerian inhibiting substance. Proc. Natl. Acad. Sci. USA 102, 111–116.

4. Bakkum-Gamez, J.N., Aletti, G., Lewis, K.A., Keeney, G.L., Thomas, B.M., Navarro-Teulon, I., and Cliby, W.A. (2008). Müllerian inhibiting substance type II receptor (MISIIR): a novel, tissue-specific target expressed by gynecologic cancers. Gynecol. Oncol. 108, 141–148.

5. Song, J.Y., Chen, K.Y., Kim, S.Y., Kim, M.R., Ryu, K.S., Cha, J.H., Kang, C.S., MacLaughlin, D.T., and Kim, J.H. (2009). The expression of Müllerian inhibiting substance/anti-Müllerian hormone type II receptor protein and mRNA in benign, borderline and malignant ovarian neoplasia. Int. J. Oncol. 34, 1583–1591.

6. Barbie, T.U., Barbie, D.A., MacLaughlin, D.T., Maheswaran, S., and Donahoe, P.K. (2003). Mullerian inhibiting substance inhibits cervical cancer cell growth via a pathway involving p130 and p107. Proc. Natl. Acad. Sci. USA 100, 15601–15606.

7. Pépin, D., Sosulski, A., Zhang, L., Wang, D., Vathipadiekal, V., Hendren, K., Coletti, C.M., Yu, A., Castro, C.M., Birrer, M.J., et al. (2015). AAV9 delivering a modified human Mullerian inhibiting substance as a gene therapy in patient-derived xenografts of ovarian cancer. Proc. Natl. Acad. Sci. USA 112, E4418–E4427.

8. Hoshiya, Y., Gupta, V., Segev, D.L., Hoshiya, M., Carey, J.L., Sasur, L.M., Tran, T.T., Ha, T.U., and Maheswaran, S. (2003). Mullerian inhibiting substance induces NFkB signaling in breast and prostate cancer cells. Mol. Cell. Endocrinol. 211, 43–49.

9. Segev, D.L., Hoshiya, Y., Hoshiya, M., Tran, T.T., Carey, J.L., Stephen, A.E., MacLaughlin, D.T., Donahoe, P.K., and Maheswaran, S. (2002). Mullerian-inhibiting substance regulates NF-κB signaling in the prostate in vitro and in vivo. Proc. Natl. Acad. Sci. USA 99, 239–244.

10. Beck, T.N., Korobeynikov, V.A., Kudinov, A.E., Georgopoulos, R., Solanki, N.R., Andrews-Hoke, M., Kistner, T.M., Pépin, D., Donahoe, P.K., Nicolas, E., et al. (2016). Anti-Müllerian hormone signaling regulates epithelial plasticity and chemoresistance in lung cancer. Cell Rep. 16, 657–671.

11. Parry, R.L., Chin, T.W., Epstein, J., Hudson, P.L., Powell, D.M., and Donahoe, P.K. (1992). Recombinant human Mullerian inhibiting substance inhibits human ocular melanoma cell lines in vitro and in vivo. Cancer Res. 52, 1182–1186.

12. Chin, T.W., Parry, R.L., and Donahoe, P.K. (1991). Human Müllerian inhibiting substance inhibits tumor growth in vitro and in vivo. Cancer Res. 51, 2101–2106.

13. Ha, T.U., Segev, D.L., Barbie, D., Masiakos, P.T., Tran, T.T., Dombkowski, D., Glander, M., Clarke, T.R., Lorenzo, H.K., Donahoe, P.K., and Maheswaran, S. (2000). Müllerian inhibiting substance inhibits ovarian cell growth through an Rb-independent mechanism. J. Biol. Chem. 275, 37101–37109.

14. Stephen, A.E., Pearsall, L.A., Christian, B.P., Donahoe, P.K., Vacanti, J.P., and MacLaughlin, D.T. (2002). Highly purified Müllerian inhibiting substance inhibits human ovarian cancer in vivo. Clin. Cancer Res. 8, 2640–2646.

15. Pieretti-Vanmarcke, R., Donahoe, P.K., Szotek, P., Manganaro, T., Lorenzen, M.K., Lorenzen, J., Connolly, D.C., Halpern, E.F., and MacLaughlin, D.T. (2006). Recombinant human Mullerian inhibiting substance inhibits long-term growth of MIS type II receptor-directed transgenic mouse ovarian cancers in vivo. Clin. Cancer Res. 12, 1593–1598.

16. Salhi, I., Cambon-Roques, S., Lamarre, I., Laune, D., Molina, F., Pugnière, M., Pourquier, D., Gutowski, M., Picard, J.Y., Xavier, F., et al. (2004). The anti-Müllerian hormone type II receptor: insights into the binding domains recognized by a monoclonal antibody and the natural ligand. Biochem. J. 379, 785–793.

17. Eng, K.H., Weir, I., Tsuji, T., and Odunsi, K. (2015). Immuno-stimulatory/regulatory gene expression patterns in advanced ovarian cancer. Genes Cancer 6, 399–407.

18. Yuan, Q.A., Robinson, M.K., Simmons, H.H., Russeva, M., and Adams, G.P. (2008). Isolation of anti-MISIIR scFv molecules from a phage display library by cell sorter biopanning. Cancer Immunol. Immunother. 57, 367–378.

19. Yuan, Q.A., Simmons, H.H., Robinson, M.K., Russeva, M., Marasco, W.A., and Adams, G.P. (2006). Development of engineered antibodies specific for the Müllerian inhibiting substance type II receptor: a promising candidate for targeted therapy of ovarian cancer. Mol. Cancer Ther. 5, 2096–2105.

20. Song, D.G., and Powell, D.J. (2012). Pro-survival signaling via CD27 costimulation drives effective CAR T-cell therapy. OncoImmunology 1, 547–549.

21. Hudecek, M., Lupo-Stanghellini, M.T., Kosasih, P.L., Sommermeyer, D., Jensen, M.C., Rader, C., and Riddell, S.R. (2013). Receptor affinity and extracellular domain modifications affect tumor recognition by ROR1-specific chimeric antigen receptor T cells. Clin. Cancer Res. 19, 3153–3164.

22. Meirelles, K., Benedict, L.A., Dombkowski, D., Pepin, D., Preffer, F.I., Teixeira, J., Tanwar, P.S., Young, R.H., MacLaughlin, D.T., Donahoe, P.K., and Wei, X. (2012). Human ovarian cancer stem/progenitor cells are stimulated by doxorubicin but inhibited by Mullerian inhibiting substance. Proc. Natl. Acad. Sci. USA 109, 2358–2363.

23. Wang, P.Y., Koishi, K., McGeachie, A.B., Kimber, M., Maclaughlin, D.T., Donahoe, P.K., and McLennan, I.S. (2005). Mullerian inhibiting substance acts as a motor neuron survival factor in vitro. Proc. Natl. Acad. Sci. USA 102, 16421–16425.

24. Posey, A.D., Jr., Schwab, R.D., Boesteanu, A.C., Steentoft, C., Mandel, U., Engels, B., Stone, J.D., Madsen, T.D., Schreiber, K., Haines, K.M., et al. (2016). Engineered CAR T cells targeting the cancer-associated Tn-glycoform of the membrane mucin MUC1 control adenocarcinoma. Immunity 44, 1444–1454.

25. Sakalar, C., Mazumder, S., Johnson, J.M., Altuntas, C.Z., Jaini, R., Aguilar, R., Naga Prasad, S.V., Connolly, D.C., and Tuohy, V.K. (2015). Regulation of murine ovarian epithelial carcinoma by vaccination against the cytoplasmic domain of anti-Müllerian hormone receptor II. J. Immunol. Res. 2015, 630287.

26. June, C.H., and Sadelain, M. (2018). Chimeric antigen receptor therapy. N. Engl. J. Med. 379, 64–73.

27. Zhang, L., Conejo-Garcia, J.R., Katsaros, D., Gimotty, P.A., Massobrio, M., Regnani, G., Makrigiannakis, A., Gray, H., Schlienger, K., Liebman, M.N., et al. (2003). Intratumoral T cells, recurrence, and survival in epithelial ovarian cancer. N. Engl. J. Med. 348, 203–213.

28. Rodriguez-Garcia, A., Minutolo, N.G., Robinson, J.M., and Powell, D.J. (2017). T-cell target antigens across major gynecologic cancers. Gynecol. Oncol. 145, 426–435.

29. Kim, J.H., MacLaughlin, D.T., and Donahoe, P.K. (2014). Müllerian inhibiting substance/anti-Müllerian hormone: a novel treatment for gynecologic tumors. Obstet. Gynecol. Sci. 57, 343–357.

30. Maus, M.V., Haas, A.R., Beatty, G.L., Albelda, S.M., Levine, B.L., Liu, X., Zhao, Y., Kalos, M., and June, C.H. (2013). T cells expressing chimeric antigen receptors can cause anaphylaxis in humans. Cancer Immunol. Res. 1, 26–31.

31. Kershaw, M.H., Westwood, J.A., Parker, L.L., Wang, G., Eshhar, Z., Mavroukakis, S.A., White, D.E., Wunderlich, J.R., Canevari, S., Rogers-Freezer, L., et al. (2006). A phase I study on adoptive immunotherapy using gene-modified T cells for ovarian cancer. Clin. Cancer Res. 12, 6106–6115.

32. Song, D.G., Ye, Q., Poussin, M., Harms, G.M., Figini, M., and Powell, D.J., Jr. (2012). CD27 costimulation augments the survival and antitumor activity of redirected human T cells in vivo. Blood 119, 696–706.

33. Kersual, N., Garambois, V., Chardès, T., Pouget, J.P., Salhi, I., Bascoul-Mollevi, C., Bibeau, F., Busson, M., Vié, H., Clémenceau, B., et al. (2014). The human Müllerian inhibiting substance type II receptor as immunotherapy target for ovarian cancer. Validation using the mAb 12G4. MAbs 6, 1314–1326.

34. Zhao, J., Song, Y., and Liu, D. (2019). Clinical trials of dual-target CAR T cells, donor-derived CAR T cells, and universal CAR T cells for acute lymphoid leukemia. J. Hematol. Oncol. 12, 17.

35. Teixeira, J., He, W.W., Shah, P.C., Morikawa, N., Lee, M.M., Catlin, E.A., Hudson, P.L., Wing, J., Maclaughlin, D.T., and Donahoe, P.K. (1996). Developmental expression of a candidate Müllerian inhibiting substance type II receptor. Endocrinology 137, 160–165.

36. Kimura, A.P., Yoneda, R., Kurihara, M., Mayama, S., and Matsubara, S. (2017). A long noncoding RNA, lncRNA-Amhr2, plays a role in Amhr2 gene activation in mouse ovarian granulosa cells. Endocrinology 158, 4105–4121.

37. Hirschhorn, T., di Clemente, N., Amsalem, A.R., Pepinsky, R.B., Picard, J.Y., Smorodinsky, N.I., Cate, R.L., and Ehrlich, M. (2015). Constitutive negative regulation in the processing of the anti-Müllerian hormone receptor II. J. Cell Sci. 128, 1352–1364.

38. Faure, E., Gouédard, L., Imbeaud, S., Cate, R., Picard, J.Y., Josso, N., and di Clemente, N. (1996). Mutant isoforms of the anti-Müllerian hormone type II receptor are not expressed at the cell membrane. J. Biol. Chem. 271, 30571–30575.

39. Imhoff, F.M., Yang, D., Mathew, S.F., Clarkson, A.N., Kawagishi, Y., Tate, W.P., Koishi, K., and McLennan, I.S. (2013). The type 2 anti-Müllerian hormone receptor has splice variants that are dominant-negative inhibitors. FEBS Lett. 587, 1749–1753.

40. Song, D.G., Ye, Q., Poussin, M., Liu, L., Figini, M., and Powell, D.J., Jr. (2015). A fully human chimeric antigen receptor with potent activity against cancer cells but reduced risk for off-tumor toxicity. Oncotarget 6, 21533–21546.

41. Godwin, A.K., Meister, A., O'Dwyer, P.J., Huang, C.S., Hamilton, T.C., and Anderson, M.E. (1992). High resistance to cisplatin in human ovarian cancer cell lines is associated with marked increase of glutathione synthesis. Proc. Natl. Acad. Sci. USA 89, 3070–3074.

42. George, E., Kim, H., Krepler, C., Wenz, B., Makvandi, M., Tanyi, J.L., Brown, E., Zhang, R., Brafford, P., Jean, S., et al. (2017). A patient-derived-xenograft platform to study BRCA-deficient ovarian cancers. JCI Insight 2, e89760.

43. Ince, T.A., Sousa, A.D., Jones, M.A., Harrell, J.C., Agoston, E.S., Krohn, M., Selfors, L.M., Liu, W., Chen, K., Yong, M., et al. (2015). Characterization of twenty-five ovarian tumour cell lines that phenocopy primary tumours. Nat. Commun. 6, 7419.

44. Lanitis, E., Poussin, M., Hagemann, I.S., Coukos, G., Sandaltzopoulos, R., Scholler, N., and Powell, D.J., Jr. (2012). Redirected antitumor activity of primary human lymphocytes transduced with a fully human anti-mesothelin chimeric receptor. Mol. Ther. 20, 633–643.